Received: 30 March 2018 | Revised: 27 June 2018 | Accepted: 28 June 2018

DOI: 10.1002/mmce.21463

WILEY INTERNATIONAL JOURNAL OF RF AND MICROWAVE COMPUTER-AIDED ENGINEERING

RESEARCH ARTICLE

Single layered swastika-shaped flexible linear-to-circular polarizer using textiles for S-band application

Hidayath Mirza[1,2] | Toufiq Md Hossain[1] | Ping Jack Soh[1] | Mohd Faizal Jamlos[1] | Muhammad Nazrin Ramli[1] | Emad S. Hassan[2] | Azremi Abdullah Al-Hadi[1] | Sen Yan[3]

[1]Advanced Communication Engineering, Center of Excellence, School of Computer and Communication Engineering, Universiti Malaysia Perlis, Arau, Perlis, Malaysia

[2]Department of Electrical Engineering, College of Engineering, Jazan University, Jazan, Kingdom of Saudi Arabia

[3]School of Electronics and Information Engineering, Xi'an Jiaotong University, Xi'an, Shaanxi, People's Republic of China

Correspondence
Ping Jack Soh, Advanced Communication Engineering, Centre of Excellence, School of Computer and Communication Engineering, Universiti Malaysia Perlis, Pauh Putra, 02600 Arau, Perlis, Malaysia.
Email: pjsoh@unimap.edu.my

Funding information
Fonds Wetenschappelijk Onderzoek, Grant/Award Number: 12O1217N; Ministry of Higher Education, Malaysia, Grant/Award Number: PRGS/2/2015/ICT06/UNIMAP/02/1

Abstract

A new swastika-shaped single layered flexible linear-to-circular polarizer is proposed for Cube Satellite application in S-band. The proposed linear-to-circular polarizer is designed fully using ShieldIt Super conductive textile on a lightweight felt substrate. Principle of operation is discussed comprehensively with an equivalent circuit model and its interaction with different orthogonal polarized wave components along with a succinct study of surface currents in different polarizations. Another linear-to-circular polarizer implemented on Polydimethylsiloxane (PDMS) substrate is designed and compared with the textile-based design. A preliminary deployment scheme is also proposed and studied by analyzing its performance under different bending conditions. Both textile and PDMS structures are confirmed to be operational within the range of 2.39 to 2.45 GHz. The textile polarizer is then prototyped and validated to be exhibiting similar conversion efficiency (CE) of 98% (simulated) and 93% (measured) at 2.45 GHz. Moreover, the fractional bandwidth defined by their 90% CE limits are 7.35% (from 2.36 to 2.55 GHz) in simulations and 6.6% (from 2.36 to 2.52 GHz) in measurements. The resulting axial ratio produced is 1.4 dB (in simulations) and 2 dB (in measurements), indicated its suitability for S-band application.

KEYWORDS

CubeSat application, linear-to-circular polarizer, S-band polarizer, textile polarizer

1 | INTRODUCTION

Cube Satellites (CubeSats), a new class of picosatellites, have established itself as an eminent cost-effective functional alternative to large satellites in the realm of space exploration.[1–4]Such satellites are sent into orbit for dedicated tasks such as imaging, monitoring, and location tracking and etc.[2,4–6] They are typically deployed in or around the low Earth orbit (LEO). A spectrum of frequencies has been assigned by Federal Communications Commission and one of the recommended bands is in the S-band, from 2.39 to 2.45 GHz,[3,7] typically used for climate observation, space weather forecasting and monitoring.[1] For CubeSats, the use of high gain antennas with stringent circular polarization (CP) characteristics is capable of enabling power efficiency. This is so that the transmitting antenna may improve the link budget required for communication with the earth station from the LEO without the use of additional amplifiers, which consumes additional power.[8,9] However, to design a CP antenna fulfilling the space constraints in CubeSat is challenging.[1] Placing a polarizer in front of antenna array producing linearly polarized waves (LPWs) to achieve CP is considered a simple alternative to full engineering design effort to independently produce high gain CP antennas.[10–12]

Due to these reasons, various linear-to-circular polarizers have been proposed for different applications, including satellite communication.[11–13] These polarizers are fundamentally formed using frequency-selective surface unit cells in the

 © 2018 Wiley Periodicals, Inc.

form of loops, meander lines, dipoles[13,14]; and also with metamaterial-based structures or resonators[15–17,20]. Their operating frequencies include the Ka-band,[8] X-band,[10,17–19] and several other frequency bands[15,16,20] to cater different applications, including space application. However, very few researches are focused on designing linear-to-circular polarizers for S-band applications, except for our initial work in Ref.[13] Moreover, most of the reported polarizers listed in Table 1 are made using rigid, high density materials, with planar array of unit cells. This hinders its implementation in a deployable format. Besides that, the multilayered configuration not only contributes to the increased thickness and complex fabrication process, but also potentially increases cost.[18] Moreover, the high density substrates may also result in added weight for the overall polarizer. On the contrary, flexible and lightweight textile-based materials, which have gained much popularity in different applications such as wearable antennas[22,23] can be used as an alternative approach. This article presents an innovative single layered linear-to-circular polarizer using flexible and lightweight textile materials. Simulations and measurements indicated good agreements, with a maximum conversion efficiency (CE) of 98.07% in simulations and 97.89% in measurements. Table 1 represents the comparison of different polarizers with the proposed design by pinpointing on the material density and number of layers. This article is organized as follows. Section 2 describes the theory of linear-to-circular polarizer and its design approach in terms of its equivalent circuit model. In Section 3, the performance of the proposed textile polarizer is assessed for flat and bent conditions, in both normal and oblique incidences in terms of CE, 3 dB axial ratio (AR) fractional bandwidth ($BW_{3\ dB}$) and phase difference. Finally, Section 4 summarizes the proposed work.

2 | THEORY AND DESIGN OF LINEAR-TO-CIRCULAR POLARIZER

2.1 | Condition for circular polarization

An LPW is impinging on the polarizer in the direction of +z-axis whose electric field E^i is polarized at α=45° is first considered. This wave can be decomposed further into two orthogonal components, E_x^i and E_y^i, representing the components of E^i toward the x- and y-axis, respectively. Meanwhile, E_x^t and E_y^t are two orthogonal components of the transmitted electric field, E^t. $\alpha = 45^\circ$ confirms maximum CP.[24] E_x^i and E_y^i have equal magnitude and phase. $T_x\left(=E_x^t/E_x^i\right)$ and $T_y\left(=E_y^t/E_y^i\right)$ are the transmission coefficients for E_x^i and E_y^i.[8,19] To enable CP, the criteria provided in Equations (1) and (2)[14,21] need to be fulfilled:

$$\left|E_x^t\right| = \left|E_y^t\right| \tag{1}$$

$$\left[\Phi_{E_x^i} + \Phi_{T_x}\right] - \left[\Phi_{E_y^i} + \Phi_{T_y}\right] = \pm n\frac{\pi}{2} \tag{2}$$

where Φ represents the phase of the respective quantity in the subscript and n = 1, 2, 3. With further simplification using $\left|E_x^i\right| = \left|E_y^i\right|$ and $\Phi_{E_x^i} = \Phi_{E_y^i}$, Equation (1) now takes form of $|T_x| = |T_y|$, while Equation (2) can be written as[14]:

$$\Phi_{T_x} - \Phi_{T_y} = 2n\pi \pm n\frac{\pi}{2} \tag{3}$$

This indicates that phase difference between T_x and T_y should be 90° or its odd multiple.

2.2 | Performance-governing parameters for linear-to-circular polarizer

Besides the CP criteria discussed in previous section, a linear-to-circular polarizer can then be assessed using (1) CE[25] as in Equation (4) and (2) AR, expressed in Equation (5).[24]

$$\eta_{conv} = \frac{\left(abs(C_-)^2 - abs(C_+)^2\right)}{\left(abs(C_-)^2 + abs(C_+)^2\right)} * 100 \tag{4}$$

$$\mathrm{AR} = \sqrt{\frac{\left|T_y\right|^2 + \left|T_x\right|^2 + \left|T_y^2 + T_x^2\right|}{\left|T_y\right|^2 + \left|T_x\right|^2 - \left|T_y^2 + T_x^2\right|}} \tag{5}$$

where C_- and C_+ are the circular conversion coefficient for the right-handed CP wave and left-handed CP wave, respectively.[21,25]

2.3 | Linear-to-circular polarizer design and principle of operation

The proposed polarizer topology shown in Figure 1 contains a conductor strip (CS) parallel to the x-axis in the front plane, and a swastika-shaped structure in the rear plane aligned with an angular value of α=45° with the +x-axis. The main design objective is to introduce capacitive effect in one component of the transmitted electric field E^t and inductive characteristic to the other component. The use of these linear-to-circular polarizer unit cells with different shapes enables the control of the

TABLE 1 Comparison of previous research in terms of density and number of layers

Reference	Substrate	Type	Band	Density (gm/cm^3)	No. of layers
[14]	Rogers RT/Duroid 5870	Rigid	Ku	2.2	1
[8]	Rogers RT/Duroid 5880	Rigid	Ka	2.2	4
[12]	Rogers RT/Duroid 5880	Rigid	K	2.2	3
[13]	Felt	Flexible	S	0.25	1
[18]	Taconic RF-35	Rigid	X	2.35	1
[19]	Arlon DiClad 880	Rigid	X	2.2	4
[21]	FR-4	Rigid	X	1.85	1
This work	Felt	Flexible	S	0.25	1

10990471x, 2018, 7, Downloaded from https://onlinelibrary.wiley.com/doi/10.1002/mmce.21463, Wiley Online Library on [02/12/2024]. See the Terms and Conditions (https://onlinelibrary.wiley.com/terms-and-conditions) on Wiley Online Library for rules of use; OA articles are governed by the applicable Creative Commons License

TABLE 2 Parameters of the textile and PDMS polarizer-unit cell

Parameter	Textile	PDMS	Parameter	Textile	PDMS
A	33.0	30.6	K	06.5	11.0
B	24.0	20.0	L	06.0	04.0
C	25.0	18.5	M	44.3	21.0
D	06.0	04.0	N	04.0	06.0
E	17.0	17.0	P_x	51.7	45.3
F	17.0	14.5	P_y	59.8	56.5
G	08.0	04.0	Q	02.0	04.0
H	06.0	04.0	R	12.5	15.0
J	17.0	14.5	S	08.0	08.0

Abbreviation: PDMS, Polydimethylsiloxane.

desired electrical characteristics in the structure to fulfill the design goals. To portray the principle of operation of the proposed polarizer, a simplified equivalent circuit model is presented in Figure 2, where x and y subscripts are used to define the x and y components, respectively. Parameter $R_{TL_{subs}}$ and R_{UC} represents the characteristics of the substrate and overall resistance of the unit cell, respectively. Meanwhile, C_x, C_y, L_x, and L_y represent the overall capacitance and inductance associated with the swastika-shaped structure along with the conductor strip (CS) in the direction indicated by the subscript. After studying the effect of different gaps and lengths on the characteristics, it can be summarized from Refs. [12] and [26] that the capacitance varies inversely proportional to the gap and directly proportional to the width of the gap

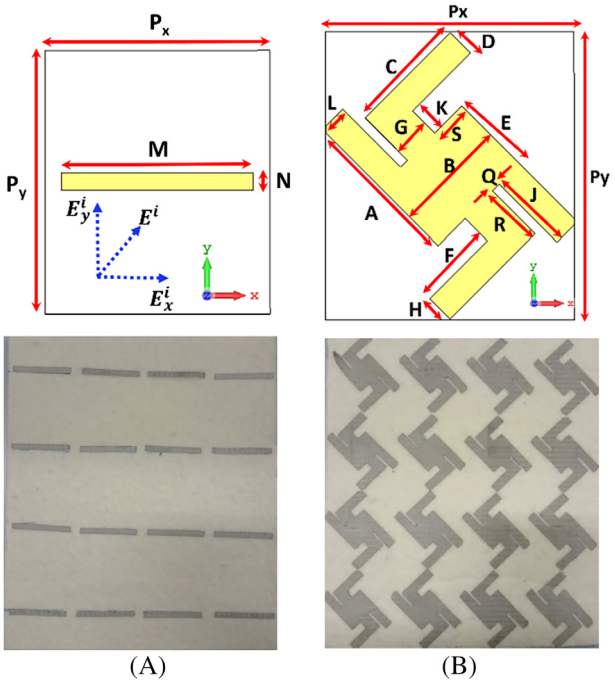


FIGURE 1 Proposed swastika-shaped linear to circular polarizer: Descriptive overview of 1 × 1 array with a size of 51.7 × 59.8 mm (top) and fabricated 4 × 4 array with a size of 206.9 × 239.2 mm (bottom) (A) front view and (B) rear view layout

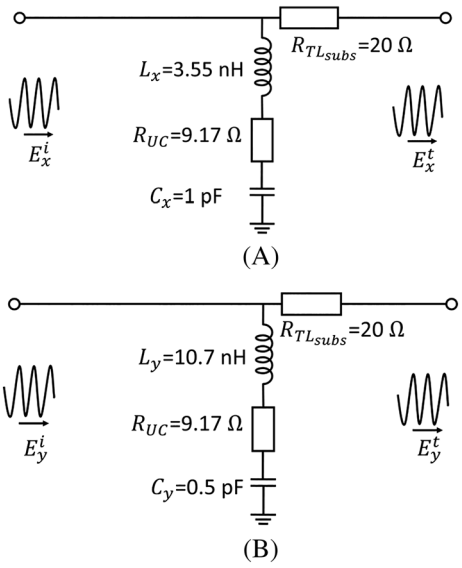


FIGURE 2 Depiction of equivalent circuit model for (A) x and (B) y polarized electric field

channel. Meanwhile, the inductance associated with the planar transmission line is directly proportional to the length of the transmission line. The smaller gap, Q, and the larger width, R, for the gap channel (as illustrated in Figure 1B top) introduce higher capacitance C_x to interact with E_x^i in the x-direction. On the other hand, the gap channel with a comparatively larger gap, K (see Figure 1B top) and smaller width, S, decreases the capacitance on E_y^i in the y-direction. Moreover, the longer length of the swastika structure in the y-direction induces additional inductance in the y-directed electric field component. As a result, the value of C_x, is larger than that of its counterpart, C_y. The inductance characteristics are designed to be of an opposite characteristic by assigning a longer length (L_y , larger than L_x) to enable larger inductance on E_y^i compared to E_x^i. Consequently, E_x^t becomes phase advanced and E_y^t achieves phase retarded characteristics. The gap and width of the channels are optimized further in terms of inductance (length) to ensure that they meet the criteria specified in Equations (1) and (2). The CS in the front plane enables further tuning without compromising the overall size of the polarizer. This CS structure introduces additional inductive characteristics for E_x^t parallel to the strip and allows the coupling of the incident wave with it. To validate the proposed equivalent circuit model, a circuit simulation has been performed using Advance Design System software, and the resulting parameter values are presented in Figure 2. In circuit simulation, it is seen that the higher value of capacitance shifts the transmission results to the higher frequency and vice versa, which is comparable with the full-wave simulation results presented in Figure 4. The working principle of the polarizer can be better explained based on the current distribution illustrated in Figure 3. The x-polarized incident wave

1099047x, 2018, 7, Downloaded from https://onlinelibrary.wiley.com/doi/10.1002/mmce.21463, Wiley Online Library on [02/12/2024]. See the Terms and Conditions (https://onlinelibrary.wiley.com/terms-and-conditions) on Wiley Online Library for rules of use; OA articles are governed by the applicable Creative Commons License

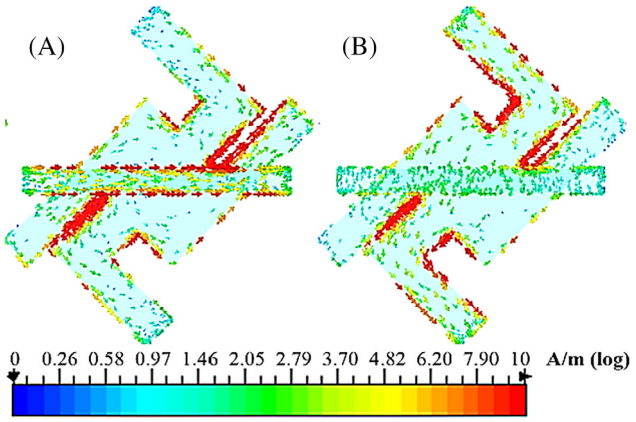


FIGURE 3 Current distributions at 2.45 GHz for (A) *x*- and (B) *y*-polarized incident electric field

directly couples to the CS, whereas the swastika-shaped structure converts part of the incident waves from the *x*-direction to the *y*-direction. Meanwhile, the *y*-polarized incident wave does not excite the CS well, resulting in a significant phase difference between the orthogonal transmitted electric field components, E_x^t and E_y^t. This phenomenon agrees well with the operation of the proposed equivalent circuit model in Figure 2.

The proposed polarizer is implemented on a felt substrate and is compared with another version designed using Polydimethylsiloxane (PDMS). The relative permittivity (ε_r) is 2.7 for PDMS and 1.44 for felt, while ShieldIt features a conductivity of 1.18×10^5 S/m with a thickness of 0.17 mm. To ensure a fair comparison between two structures, the height of the structures was kept at 3 mm, whereas the conductive textile was optimized to ensure both (PDMS and felt) operate on same frequency. The polarizer has been designed and optimized using commercially available electromagnetic simulator, CST Microwave Studio[27] using the unit cell boundary condition in the *x*- and *y*-directions. Frequency-domain solver is used with adaptive meshing for these analyses.

3 | POLARIZER ASSESSMENT AND PERFORMANCE

3.1 | Polarizer assessment

The results of proposed polarizers are shown in Figures 4–6. These results indicated a simulated phase difference and CE of 80.2° and 95.78% (for the textile-based polarizer), and 81° and 96.8% (for the PDMS-based polarizer) at 2.4 GHz. Besides that, the fractional bandwidth covering at least 90% of CE, BW_{CE} is 7.35% (from 2.36 to 2.54 GHz for textile) and 5.02% (from 2.33 to 2.45 GHz for PDMS) in simulations. This motivated the reason of choosing the textile

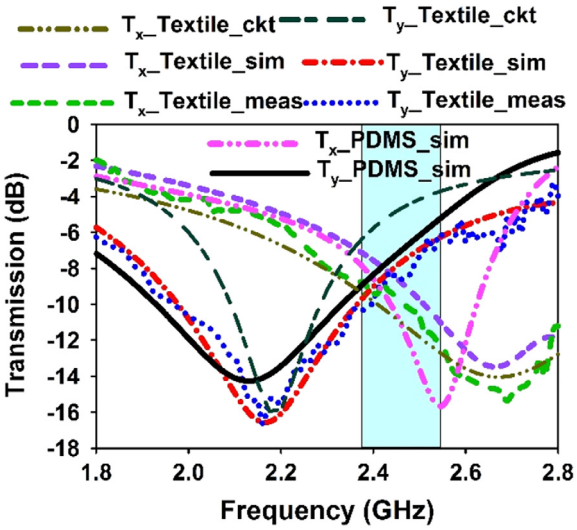


FIGURE 4 Transmission coefficients (in dB) for the proposed polarizer

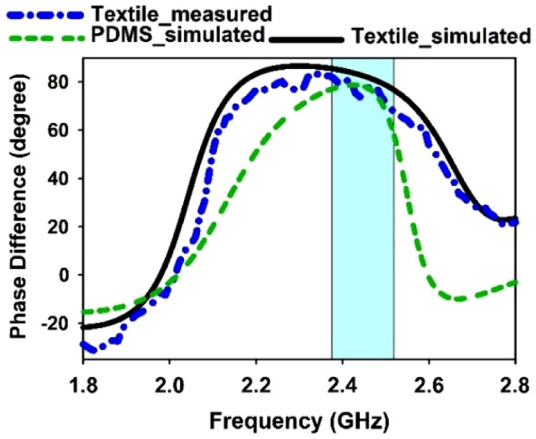


FIGURE 5 Phase difference of the proposed polarizer

prototype for further analysis of oblique incidence and to be fabricated for further assessment.

Measurements were conducted by placing the proposed polarizer between two identical horn antennas (A-INFOMW [0.8-18 GHz]). A Styrofoam structure was used to ensure a flat operating condition of the proposed polarizer during the measurement process. Parameters of the transmission coefficients (T_x and T_y) were collected for the *x* and *y* polarization by rotating the horn antennas to be polarized toward the respective direction. An Agilent E5071C network analyzer is used to gather T_x and T_y measurements between 1.8 and 2.8 GHz. These measurements are then used to calculate CE and AR using the equations described in Section 2.1.

Measurements of the phase difference and CE for the fabricated textile-based prototype are 78.3° and 97.89% at 2.4 GHz, respectively. On the other hand, a 6.56% (from 2.36 to 2.52 GHz) of measured BW_{CE} is observed for the textile-based polarizer prototype. The measurement setup is illustrated in Figure 7, and is defined based on the procedure described in Refs. 13 and 28.

10990471x, 2018, 7, Downloaded from https://onlinelibrary.wiley.com/doi/10.1002/mmce.21463, Wiley Online Library on [02/12/2024]. See the Terms and Conditions (https://onlinelibrary.wiley.com/terms-and-conditions) on Wiley Online Library for rules of use; OA articles are governed by the applicable Creative Commons License

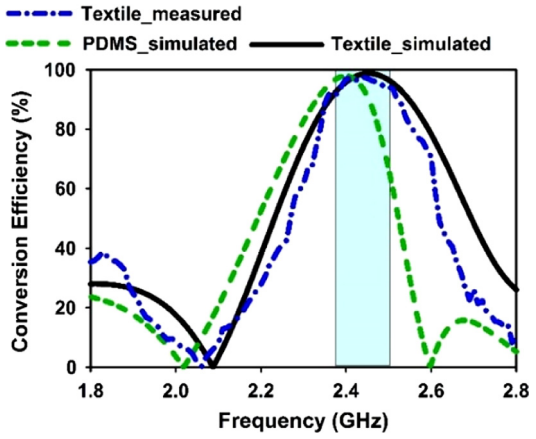


FIGURE 6 Conversion efficiency of the proposed polarizer

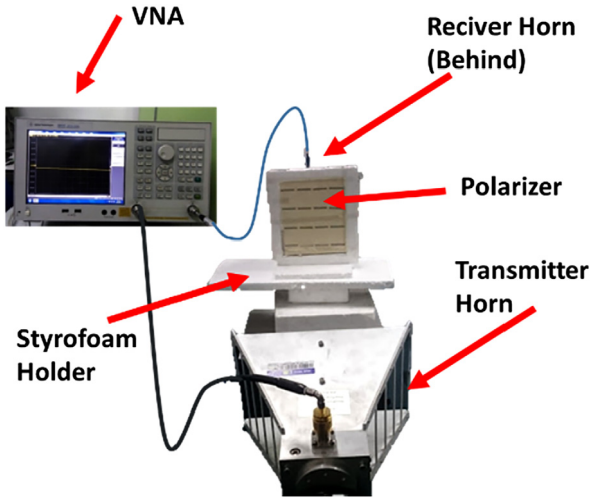


FIGURE 7 Measurement setup

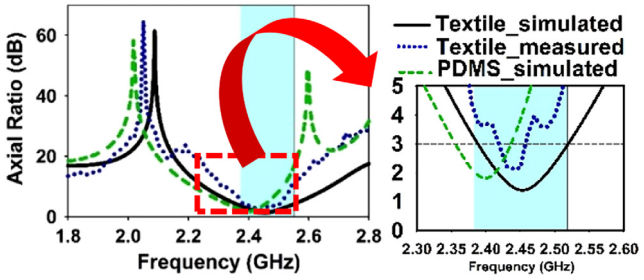


FIGURE 8 Axial ratio of the proposed polarizer

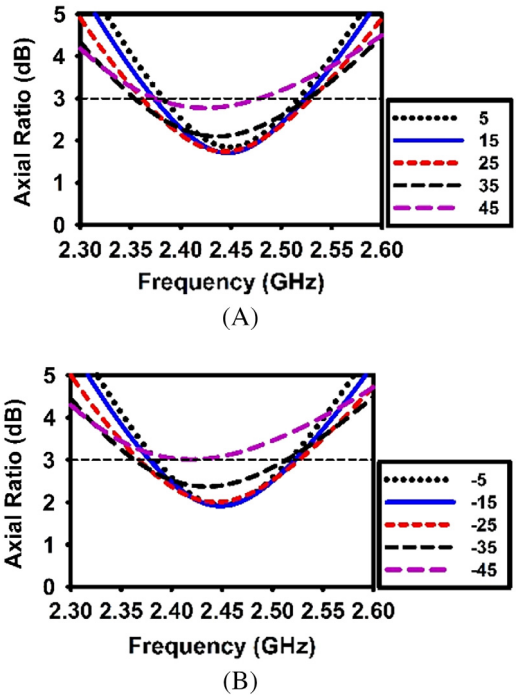


FIGURE 9 Axial ratio of the proposed textile polarizer in oblique incidence for (A) positive and (B) negative angle of incidence (θ)

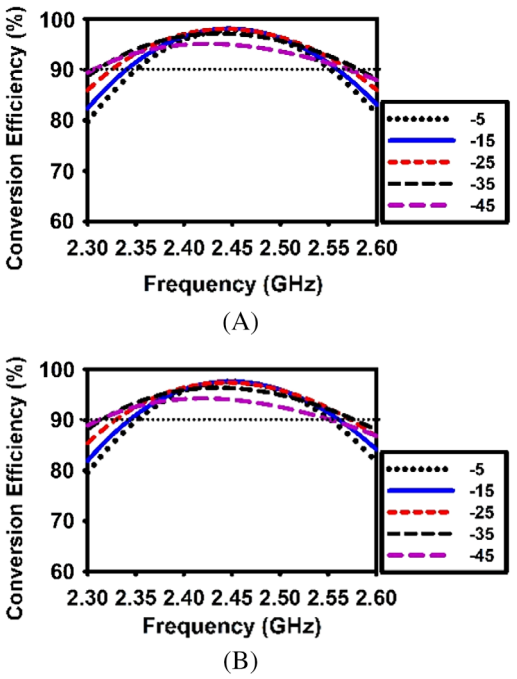


FIGURE 10 Conversion efficiency of the proposed textile polarizer in oblique incidence for (A) positive (B) negative angle of incidence (θ)

3.2 | Polarizer performance

3.2.1 | Performance in flat condition and normal incidence

As mentioned earlier, Figures 4–6 describe the results of the proposed polarizer in flat condition with normal incidence. As explained in Section 2.2, the magnitude of T_x and T_y components are required to be equal, with a ±90° phase difference based on Equation (2). It is observed in Figure 4 that all simulated and measured T_x and T_y intersections for both prototypes are within the target frequency band of 2.39 to 2.45 GHz indicating equal magnitude. Figure 5 depicts the phase difference between T_x and T_y, indicating 85° at 2.39 GHz and 82.4° at 2.45 GHz for the textile prototype (in simulation). In comparison, the PDMS exhibited a lower simulated phase difference of 78° (at 2.39 GHz) and 78.16° (at 2.4 GHz). Meanwhile, measurements of the textile-based prototype indicated a phase difference of 79.58° at 2.39 GHz and 75.4° at 2.45 GHz. Figure 6 illustrates the CE of the proposed polarizer over frequency with

10990471x, 2018, 7, Downloaded from https://onlinelibrary.wiley.com/doi/10.1002/mmce.21463, Wiley Online Library on [02/12/2024]. See the Terms and Conditions (https://onlinelibrary.wiley.com/terms-and-conditions) on Wiley Online Library for rules of use; OA articles are governed by the applicable Creative Commons License

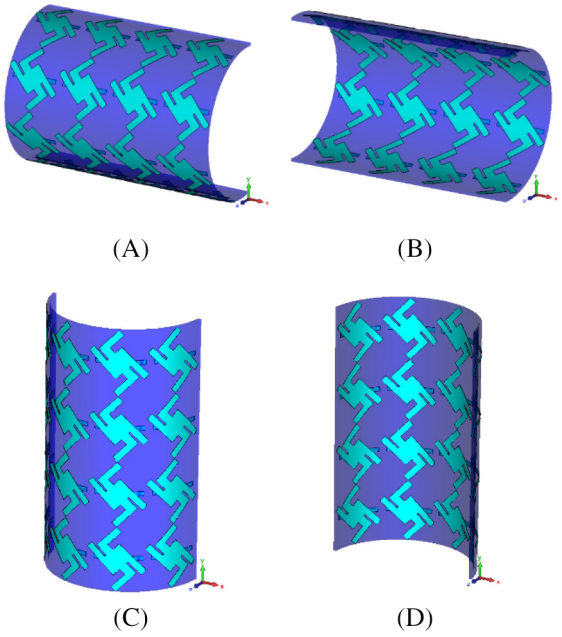


FIGURE 11 Conformal (bent) geometry of the proposed textile polarizer: top: *x*-axis bending (A) inward, and (B) outward; bottom: *y*-axis bending (C) inward, and (D) outward

its operating region (BW_{CE}) highlighted in light blue. Simulations indicated a CE of 94.55% at 2.39 GHz and 98.72% at 2.45 GHz, whereas its measured values are slightly degraded, with 94.64% at 2.39 GHz and 91.95% at 2.45 GHz. In comparison, the simulated PDMS polarizer exhibited a simulated efficiency of 97.78 and 91.37% at 2.39 and 2.45 GHz, respectively. All ARs are calculated using Equation (5) and plotted in Figure 8. Simulations indicated a minimum AR of 1.4 dB for the textile-based polarizer and 1.8 dB for the PDMS-based based polarizer. The fractional bandwidth fulfilling $AR \leq 3$ dB is 5.39% (2.39-2.52 GHz) in simulation while 1.64% (2.42-2.46 GHz) in measurement. When measured, the textile-based polarizer is slightly degraded in terms of AR to about 2 dB.

Meanwhile for the PDMS-based design, simulations indicated a minimum AR of 1.4 dB. The degradation in measurements can be attributed to the use of the finite element array in practice, whereas infinite element array is set up in simulations to save time and computational resources. Nonetheless, the simulations are in a reasonably good agreement with measurements. This meets the required maximum 3 dB condition at the desired frequencies for proper operation as a linear-to-circular polarizer. Moreover, the simulations are also in good agreement with measurements.

3.2.2 | Performance in flat condition and oblique incidence

The performance of the polarizer has been investigated in oblique incidence by varying the angle, θ, in CST Microwave Studio within $\pm 45°$ in 10° steps. This range is chosen considering the asymmetric structure in the *yz* plane. The result of AR and CE with different angles of incidence is presented in Figures 9 and 10, respectively. It can be observed that the performance of the polarizer (with AR $\leq$3 dB and with CE $\geq$90%) is stable from $\theta = 0°$ to $\theta = \pm 35°$, and only starts degrading sharply when exceeding $\theta \geq \pm 35°$. This scenario can be explained from the current distribution (in Figure 3) and the equivalent circuit model. In the case of $\theta \geq \pm 35°$, the CS is less excited due to the minimal coupling of the incident wave to it, leading to lesser inductance for E_x^t. This, in turn, affects the CP characteristics of the overall structure. However, it is expected that the integrated deployment mechanism will not result misdeployment to result in the polarizer operating with angles of incidence exceeding $\pm 35°$.

3.2.3 | Performance in conformal (bent) geometry

Due to the use of flexible materials, there exists a risk that the polarizer will not be perfectly planar when deployed. The effect of this must be studied to ensure that the level of degradation due to this slight bending is quantified. A series of investigations of the textile-based polarizer operating under bent condition is performed, as illustrated in Figure 11. It is bent over a hypothetical cylinder with radius of 70 mm in both the *x*- and *y*-axis. For each axis, bending toward the $+z$-axis is denoted as the inward bending, and bending toward the $-z$-axis is denoted as the outward bending. Its performance in terms of phase difference and CE is

TABLE 3 Performance summary of the polarizer when operated in planar and bent conditions

				Bent			
				Inward		Outward	
Parameter		**Frequency (GHz)**	**Flat**	***x*-axis**	***y*-axis**	***x*-axis**	***y*-axis**
Phase difference (°)	Simulated	2.39	85	37.55	35.47	92.64	22.43
		2.45	82.40	53.31	31.98	90.392	9.585
	Measured	2.39	79.58	N/A			
		2.45	75.40				
CE (%)	Simulated	2.39	94.55	37.18	55.74	87.07	36.77
		2.45	98.72	65.46	50.47	70.62	16.33
	Measured	2.39	94.64	N/A			
		2.45	91.95				

Abbreviation: CE, conversion efficiency.

1099047x, 2018, 7, Downloaded from https://onlinelibrary.wiley.com/doi/10.1002/mmce.21463, Wiley Online Library on [02/12/2024]. See the Terms and Conditions (https://onlinelibrary.wiley.com/terms-and-conditions) on Wiley Online Library for rules of use; OA articles are governed by the applicable Creative Commons License

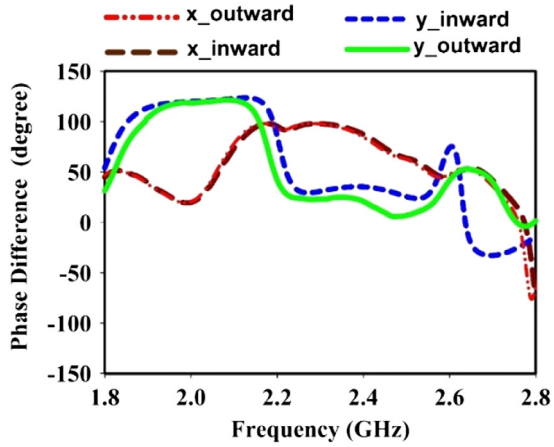


FIGURE 12 Phase difference of the in conformal (bent) condition

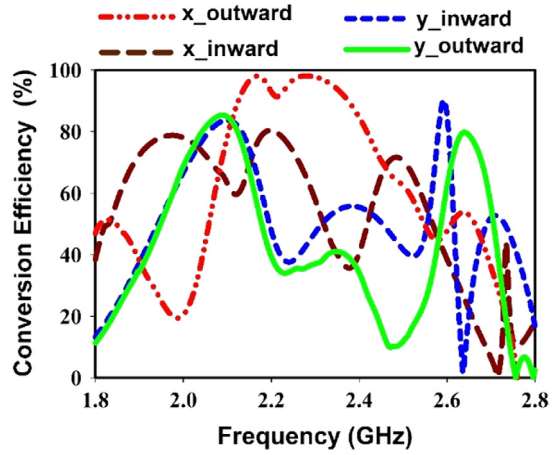


FIGURE 13 Conversion efficiency of the polarizer in conformal (bent) condition

paralleled with flat condition results in Table 3. Figure 11 depicts the conformal (bent) geometry of the 4 × 4 polarizer in bent condition while the phase characteristics are shown in Figure 12. In general, bending at the *x*-axis (both outward and inward) indicated no significant difference in terms of phase difference. Meanwhile, larger changes in terms of CE are seen when the polarizer is bent at the *y*-axis within the S-band, see Figure 13. Despite the poor performance when bent at the *y*-axis, it is observed that the inward bending resulted in a relatively higher CE compared to when bent outward. On the other hand, it is found that the *x*-axis outward bending provided the best efficiency within S-band. This study also provides several cues on the precautionary steps in ensuring a fail-safe design for the proposed linear-to-circular polarizer. First, the mounting of mechanical deployable structure must be done in a way that its imperfect deployment should result in the more favorable conformal configuration (in this case, toward the *x*-axis, with outward bend). Finally, a halting mechanism (or a simple stopper) needs to be integrated with the deployment structure to avoid the proposed polarizer to be deployed toward its worst-performing condition (bent outward or inward at the *y*-axis).

4 | CONCLUSION

In this work, an innovative linear-to-circular polarizer fully designed and implemented using textiles are proposed for CubeSat application in the S-band. Commercially available lightweight textile material, felt and ShieldIt, are used to ensure polarizer's flexibility and ease of deployment process to overcome space limitations in CubeSats. A comprehensive operating principle is presented with the aid of a generalized equivalent circuit model and current distribution. Moreover, oblique incidence results have been investigated to characterize the maximum oblique angle and it is found to be stable within a range from 0° to ±35° in terms of AR and conversion coefficient. Different bending conditions are assessed in terms of the phase difference and CE to provide further understanding of its performance when used in practice. Under different *x*-axis bending conditions, a robust performance is observed, thus resulting in a set of precautionary steps to be taken when implementing it onto the mechanical deployment structure. Measurements of the fabricated textile prototype indicated good agreements with simulations, with a measured CE of more than 92% and AR of 2 dB in the S-band.

ACKNOWLEDGMENTS

This project was supported in part the Malaysian Ministry of Higher Education (MOHE) Prototype Development and Research Grant Scheme (PRGS) (grant no: PRGS/2/2015/ICT06/UNIMAP/02/1) and Research Foundation Flanders (FWO) Postdoctoral Fellowship (No. 12O1217N). The technical contributions by Abdul Halim Lokman and Rizwan Khan Jadoon are also acknowledged.

ORCID

Toufiq Md Hossain http://orcid.org/0000-0001-6621-5555
Ping Jack Soh http://orcid.org/0000-0002-6394-5330

REFERENCES

1. Lokman AH, Soh PJ, Azemi SN, et al. A review of antennas for picosatellite applications. *Int J Antennas Propag*. 2017;2017:1-17.
2. Hodges RE, Hoppe DJ, Radway MJ, Chahat NE. Novel deployable reflectarray antennas for CubeSat communications. In: IEEE MTT-S International Microwave Symposium; 2015:4-7, Phoenix, AZ, USA.
3. V. Shirvante, S. Johnson, K. Cason, K. Patankar, and N. G. Fitz-Coy, Configuration of 3U CubeSat structures for gain improvement of S-band antennas. [Online]. https://digitalcommons.usu.edu/smallsat/2012/all2012/73/. Accessed August 11, 2017.
4. Chahat N, Hodges RE, Sauder J, Thomson M, Rahmat-Samii Y. The deep-space network telecommunication CubeSat antenna: using the deployable Ka-band mesh reflector antenna. *IEEE Antennas Propag Mag*. 2017;59(2):31-38.
5. C. J. Vourch and T. D. Drysdale, Inter-CubeSat communication with V-band Bull's Eye Antenna. In: The 8th European Conference on Antennas and Propagation (EuCAP 2014); 2014:3545-3549, The Hague, Netherlands.
6. N. Chahat, R. Hodges, J. Sauder, M. Thomson, and Y. Rahmat-Samii, Earth science RADAR CubeSat deployable Ka-band mesh reflector antenna. 2016 I.E. International Symposium on Antennas and Propagation (APSURSI), vol. 64, no. 6; 2016:1531-1532, Fajardo, Puerto Rico.
7. Federal Communications Commision (FCC), Guidance on obtaining licenses for small satellites. [Online]. https://www.fcc.gov/document/guidance-obtaining-licenses-small-satellites. Accessed January 26, 2018.

10990471x, 2018, 7, Downloaded from https://onlinelibrary.wiley.com/doi/10.1002/mmce.21463, Wiley Online Library on [02/12/2024]. See the Terms and Conditions (https://onlinelibrary.wiley.com/terms-and-conditions) on Wiley Online Library for rules of use; OA articles are governed by the applicable Creative Commons License

8. Martinez-Lopez L, Rodriguez-Cuevas J, Martinez-Lopez JI, Martynyuk AE. A multilayer circular polarizer based on bisected split-ring frequency selective surfaces. *IEEE Antennas Wirel Propag Lett*. 2014;13:153-156.
9. Babuscia A, Corbin B, Knapp M, Jensen-Clem R, Van De Loo M, Seager S. Inflatable antenna for cubesats: motivation for development and antenna design. *Acta Astronaut*. 2013;91:322-332.
10. Fartookzadeh M, Armaki SHM. Dual-band reflection-type circular polarizers based on anisotropic impedance surfaces. *IEEE Trans Antennas Propag*. 2016;64(2):826-830.
11. Ranga Y, Matekovits L, Hay SG, Bird TS. An anisotropic impedance surface for dual-band linear-to-circular transmission polarization converter. 2013 International Workshop on Antenna Technology, iWAT, vol. 91; 2013:322-332, Karlsruhe, Germany.
12. Hosseini M, Hum SV. A circuit-driven design methodology for a circular polarizer based on modified Jerusalem cross grids. *IEEE Trans Antennas Propag*. 2017;65(10):5322-5331.
13. Mirza H, Soh PJ, Jamlos MF, et al. A crossed dodecagonal deployable polarizer on textile and polydimethylsiloxane (PDMS) substrates. *Appl Phys A*. 2018;124(2):178.
14. I. Sohail, Y. Ranga, K. P. Esselle, and S. G. Hay, A linear to circular polarization converter based on jerusalem-cross frequency selective surface. 2013 7th European Conference on Antennas and Propagation (EuCAP); 2013: 2141–2143, Gothenburg, Sweden.
15. Xu HX, Wang GM, Liang JG, Qi MQ, Gao X. Compact circularly polarized antennas combining meta-surfaces and strong space-filling meta-resonators. *IEEE Trans Antennas Propag*. 2013;61(7):3442-3450.
16. Xu HX, Wang GM, Qi MQ. A miniaturized triple-band metamaterial antenna with radiation pattern selectivity and polarization diversity. *Prog Electromagn Res*. 2013;137:275-292.
17. Xu H-X, Wang G-M, Qi MQ, Cai T, Cui TJ. Compact dual-band circular polarizer using twisted Hilbert-shaped chiral metamaterial. *Opt Express*. 2013;21(21):24912-24921.
18. Doumanis E, Goussetis G, Gómez-Tornero JL, Cahill R, Fusco V. Anisotropic impedance surfaces for linear to circular polarization conversion. *IEEE Trans. Antennas Propag*. 2012;60(1):212-219.
19. Zhang W, Li J, Wang L. Broadband circular polarizer based on multilayer gradual frequency selective surfaces. *Int J Antennas Propag*. 2016;2016:1-5.
20. Xu HX, Sun S, Tang S, et al. Dynamical control on helicity of electromagnetic waves by tunable metasurfaces. *Sci Rep*. 2016;6:1-10.
21. Yan S, Vandenbosch GAE. Compact circular polarizer based on chiral twisted double split-ring resonator. *Appl Phys Lett*. 2013;102(10):1-5.
22. Soh PJ, Vandenbosch GAE, Mercuri M, Schreurs DMMP. Wearable wireless health monitoring: current developments, challenges, and future trends. *IEEE Microw Mag*. 2015;16(4):55-70.
23. Jais MI, Bin Jamlos MF, Jusoh M, et al. A novel 2.45 GHz switchable beam textile antenna (SBTA) for outdoor wireless body area network (WBAN) applications. *Prog Electromagn Res*. 2013;138:613-627.
24. Baena JD, Glybovski SB, Del Risco JP, Slobozhanyuk AP, Belov PA. Broadband and thin linear-to-circular polarizers based on self-complementary zigzag metasurfaces. *IEEE Trans Antennas Propag*. 2017;65(8):4124-4133.
25. Wang J, Shen Z, Wu W, Feng K. Wideband circular polarizer based on dielectric gratings with periodic parallel strips. *Opt Express*. 2015;23(10):12533-12543.
26. Hosseini M, Hakkak M. Characteristics estimation for Jerusalem cross-based artificial magnetic conductors. *IEEE Antennas Wirel Propag Lett*. 2008;7:58-61.
27. CST-Computer Simulation Technology. [Online]. https://www.cst.com/. Accessed March 30, 2018.
28. Fei P, Shen Z, Wen X, Nian F. A single-layer circular polarizer based on hybrid meander line and loop configuration. *IEEE Trans Antennas Propag*. 2015;63(10):4609-4614.

AUTHOR BIOGRAPHIES



Hidayath Mirza was born in Hyderabad, India. In 2005, he received his bachelor's degree in electronics and communication engineering from Jawaharlal Nehru Technological University (JNTU), Hyderabad, India. He completed his MS in radio engineering from Kyung Hee University (KHU), South Korea in 2008 with 2 years of KHU President Scholarship. He is currently working toward his PhD degree in School of Computer and Communication Engineering, Universiti Malaysia Perlis (UniMAP), Malaysia. From 2009 to 2011, he was a full time researcher at ESAT-TELEMIC Research Division, KU Leuven, Belgium. From 2012, he was working as a lecturer at the department of electrical engineering, Jazan University, Jazan, Kingdom of Saudi Arabia. His research interests include wearable antennas, RF energy scavenging using rectenna, RFID tag antenna design, characterization of materials; extraction of permittivity, metamaterials, and flexible linear-to-circular polarizers. He was a recipient of the Young Scientist Travel Grant (YSTG), 2007 International Symposium on Antennas and Propagation (ISAP).



Toufiq Md Hossain, a Bangladeshi national, was born in Al-Kharj, Kingdom of Saudi Arabia, in 1991. He received his BSc degree in electrical and electronic engineering from Khulna University of Engineering & Technology (KUET), Khulna, in 2014. He is currently working as a research assistant in Advanced Communication Engineering (ACE), Centre of Excellence in Universiti Malaysia Perlis and on the verge of completing his MSc degree in communication engineering from the same university. He has authored or coauthored two referred journals and five international conferences. His research interests include metamaterials, flexible linear to circular polarizers for CubeSat applications and five port reflectometers, and microwave imaging of brain injury diagnosis applications.



Ping Jack Soh was born in Sabah, Malaysia. He received his BE and ME degrees from Universiti Teknologi Malaysia, and his PhD degree from KU Leuven, Belgium. He is currently an associate professor at the School of Computer and Communication Engineering, Universiti Malaysia Perlis (UniMAP), and a research affiliate at KU Leuven. From 2002 to 2004, he was a test engineer in Venture Corp., and worked in Motorola Solutions as an R&D Engineer in 2005. From 2006, he was a lecturer in UniMAP before joining the ESAT-TELEMIC Research Division, KU Leuven as a research assistant (2009-2013) and a Postdoctoral Fellow (2013-2014). Dr Soh was the recipient of the IEEE AP-S Doctoral Research Award in 2012, the IEEE MTT-S Graduate Fellowship in 2013, and the URSI Young Scientist Award in 2015. He is a chartered engineer; Senior Member of the IEEE; and Member of IET and URSI.

1099047x, 2018, 7, Downloaded from https://onlinelibrary.wiley.com/doi/10.1002/mmce.21463, Wiley Online Library on [02/12/2024]. See the Terms and Conditions (https://onlinelibrary.wiley.com/terms-and-conditions) on Wiley Online Library for rules of use; OA articles are governed by the applicable Creative Commons License



MOHD FAIZAL JAMLOS received his PhD degree in 2010 from Universiti Teknologi Malaysia, Johor, Malaysia and MSc degree in 2008 from University of Adelaide, South Australia, Australia. He is currently an associate professor at Advanced Communication Engineering Centre (ACE), School of Computer and Communication Engineering, Universiti Malaysia Perlis. He has (co-)authored some 220 scientific publications in peer-reviewed journals and conferences. His research interests include wireless embedded system, remote sensing, on-platform antennas, and microwave circuitry. He is a practice professional engineer of Board of Engineers Malaysia (BEM), Senior Member of IEEE, a National Medical Researcher (NMRR), and Corporate Member of Institute Engineers Malaysia (MIEM).



MUHAMMAD NAZRIN RAMLI was born in Perak, Malaysia, in 1991. He received his bachelor's degree in communication engineering from Universiti Malaysia Perlis (UniMAP), in 2015. He is currently working toward his MS degree in communication engineering at the School of Computer and Communication Engineering, UniMAP, Arau, Perlis, Malaysia. He is a researcher at the Advanced Communication Engineering Centre, UniMAP. His research interests include antenna and propagation, wearable antenna, flexible antenna, polymer antenna, and on-body communication. Muhammad Nazrin was a recipient at a First Place in the IEEE Malaysia Section Final Year Project Competition (Telecommunication Track) in 2015. He is also a graduate engineer of the Board of Engineers Malaysia.



EMAD S. HASSAN received his BSc (Honors), MSc, and PhD from the faculty of electronic engineering, Menoufia University, Egypt, in 2003, 2006, and 2010, respectively. He joined the teaching staff of the department of electronics and electrical communications, faculty of electronic engineering, Menoufia University, Egypt, in 2010. In 2008, he joined the communications research group at Liverpool University, Liverpool, United Kingdom, as a visitor researcher. His current research areas of interest include image processing, digital communications, cooperative communication, cognitive radio networks, OFDM, SC-FDE, MIMO, and CPM-based systems.



AZREMI ABDULLAH AL-HADI was born in Michigan, United States. He received his Master of Science degree in communication engineering from Birmingham University, United Kingdom in 2004 and his doctor of science in technology degree from Aalto University, Finland in 2013. His current research interests include design and performance evaluation of multielement antennas, mobile terminal antennas, and their user interactions. He is currently working as an associate professor at the School of Computer and Communication Engineering, Universiti Malaysia Perlis (UniMAP). He is an active volunteer with IEEE Malaysia Section, acting as the Senior Member of IEEE, Vice-Chair of the IEEE Antenna Propagation/Microwave Theory and Techniques/Electromagnetic Compatibility (AP/MTT/EMC) Malaysia Chapter and also as Counselor for IEEE UniMAP Student Branch. He was the recipient of the Best Student Paper Award presented at the 5th Loughborough Antennas and Propagation Conference (LAPC 2009) and the CST University Publication Award in 2011.



SEN YAN received his bachelor and master degrees in information and telecommunication engineering from Xi'an Jiaotong University (XJTU), China, in 2007 and 2010, respectively, and his PhD degree in electrical engineering from KU Leuven, Belgium in 2015. He was then a postdoctoral research fellow in the same institute. He obtained "Young Talent Support Plan" of XJTU, China in 2017, and is currently a full professor. Yan's research is focused on microwave metamaterials and metasurfaces, wearable devices, and textile antennas. He has authored 32 international journal papers and 27 conference contributions. He was successful in obtaining Postdoctoral Fellowships from KU Leuven and FWO in 2015 and 2016, respectively. In February 2016, he was a visiting scholar in EPFL, Switzerland, supported by COST. In August and September 2016, he was a visiting researcher in the University of Texas at Austin, United States, funded by the FWO Travel Grant.

How to cite this article: Mirza H, Hossain TM, Soh PJ, et al. Single layered swastika-shaped flexible linear-to-circular polarizer using textiles for S-band application. *Int J RF Microw Comput Aided Eng*. 2018;28:e21463. https://doi.org/10.1002/mmce.21463

1099047x, 2018, 7, Downloaded from https://onlinelibrary.wiley.com/doi/10.1002/mmce.21463, Wiley Online Library on [02/12/2024]. See the Terms and Conditions (https://onlinelibrary.wiley.com/terms-and-conditions) on Wiley Online Library for rules of use; OA articles are governed by the applicable Creative Commons License